JOURNAL OF MATERIALS SCIENCE **26** (1991) 1216–1222

Effect of temperature on interfacial shear strengths of SiC–glass interfaces

H. M. CHOU, M. W. BARSOUM, M. J. KOCZAK
Department of Materials Engineering, Drexel University, Philadelphia, PA 19104, USA

The *in situ* temperature dependencies of both the debonding, τ_d, and frictional, τ_f, shear stresses of a C-coated 140 μm SiC monofilament (Textron SCS-6 SiC fibre) were measured using the single fibre pullout-test. Two matrices, a borosilicate (7740 Corning Glass) and a soda-lime (Thomas Scientific) with different thermal expansion coefficients, were tested. At lower temperatures both τ_d and τ_f were found to decrease linearly with increasing temperature as a result of the relaxation of the residual stresses developed during processing, which were compressive in both cases. The stress free debonding shear stress for the borosilicate matrix was found to be 3.5 ± 1 MPa and the friction coefficient between that matrix and the fibres was calculated to be 0.18. Fibre oxidation are believed to be responsible for enhanced bonding between the fibres and the borosilicate matrix at higher temperatures which results in an increase in both τ_d and τ_f. The large thermal expansion mismatch between the soda-lime matrix and the SiC fibres resulted in radial cracking of the former during processing. A technique is described where the whole temperature dependence of the interfacial shear stresses can be measured by a single specimen.

1. Introduction

The mechanical properties of ceramic–matrix composites, CMCs, are strongly influenced by the debonding and frictional resistance of the interfacial area. For instance, it is well established that strong interfacial bonds between fibres and matrix will result in catastrophic failure of fibre-reinforced CMC. Weak interfaces, on the other hand, promote a more graceful failure mode and larger apparent strains to failure. The factors affecting the resistance to debond and slip are the extent of chemical bonding between fibre and matrix and the presence of residual stresses due to mismatches in thermal and elastic properties of the fibre and matrix.

One of the major impetus for developing fibre reinforced CMCs is their potential use at high temperatures. Since thermal stresses are a function of temperature, understanding the latter's effect on the interfacial properties, and ultimately on composite properties, is essential in proper design of these composites.

The methods that have been used to characterize interfacial properties are several and include measuring the saturation spacing of matrix cracks in unidirectional fibre reinforced composites [1], fibre indentation push-in [2, 3] and indentation push-out [4, 5]. For the sake of brevity these will not be discussed here. More details concerning these techniques can be found in a recent review article [6].

An alternative method, originally developed for fibres in polymer matrix composites [7], but which has recently been used for brittle matrices [8–11], is to measure the force required to pull out a single fibre partially embedded in a matrix. A typical load displacement curve for such a test, shown in Fig. 1, exhibits a peak load followed by a more gradually decreasing load as the fibre pulls out. The peak load, F_d, is usually related to a debonding mechanism where it is assumed that any chemical bonds between fibre and matrix are severed. The lower load, F_f, is associated with frictional resistance to fibre pullout.

These loads can be related to an interfacial shear stress; the exact relationship, however, depends on the model used. If the shear stress acting along the interface is assumed constant, the interfacial shear strengths, whether debonding, τ_d, or frictional, τ_f, are related to the load according to:

$$\tau_d = \frac{F_d}{2\pi r l_e} \qquad (1)$$

or

$$\tau_f = \frac{F_f}{2\pi r l_e} \qquad (2)$$

where r is the fibre radius and l_e the embedded length.

Alternatively, if the normal stress in the matrix is negligible relative to the fibre and the shear stress in the fibre is small with respect to the matrix it can be shown that [12]:

$$\tau_d = \frac{\beta F_d}{2\pi r \tanh(\beta L)} \qquad (3)$$

and

$$F_f = \frac{\pi r^2 \sigma_r}{K}\left[1 - \exp\left(-\frac{2\mu K l_e}{r}\right)\right] \qquad (4)$$

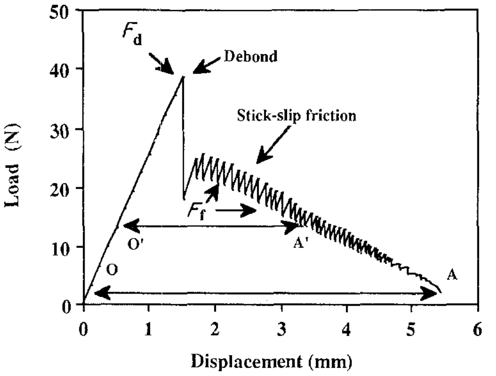

Figure 1 Typical load against displacement curve for SiC–soda-lime glass specimen. Instantaneous embedded length (after debond) at any load F is the difference between the total embedded length and the pullout length, i.e. OA–O′A′.

where β is a shear-lag parameter that depends on the details of the model used [13]. μ and σ_r are, respectively, the friction coefficient and the radial compressive residual stress at the interface. K is defined as $K = E_m v_m / E_f(1 + v_f)$ where E_i and v_i refer to the elastic constants and Poisson's ratios of the fibres and matrix. τ_d is determined from Equation 3 by performing the pullout over a range of l_e and carrying out a non-linear regression analysis from which the values of α and $(2\tau_d/r\alpha)$ are calculated. Similarly a non-linear regression best fit of F_f versus l_e is used to estimate the values of the two constants $\pi r^2 \sigma_r K$ and $2\mu K r$. The product of these two constants divided by the fibre circumference yields $\tau_f(\tau_f = \sigma_r \mu)$.

For fibres that are residually stressed the shear stress can be described as the sum of two terms [14]:

$$\tau_d = \tau_0 + \tau_f = \tau_0 + \sigma_r \mu \qquad (5)$$

where τ_0 is the stress-free interfacial shear strength. Varying the temperature varies the residual stress field, σ_r, resulting in a variation in τ_f.

The main purpose of this work was to study the effect of temperature on both τ_d and τ_f in single fibre-pullout tests. Soda-lime and borosilicate glasses were chosen as the matrices with a C-coated SiC monofilament as the fibre.

The interfacial shear stresses for SiC monofilaments embedded in borosilicate glasses have been measured using the single fibre pullout test [8–11]. The values at ambient temperatures range from 5–7.5 MPa for τ_d, and 3.5–4.5 MPa for τ_f. Goettler and Faber [10, 11] studied the effect of residual stresses by altering the thermal expansion mismatch between fibre and matrix. τ_d for a glass composition with a thermal expansion closest to the borosilicate composition used here and by others [10, 11] (i.e. CGW 7740) was found to be 17 MPa. τ_f, on the other hand, was measured to be 4.5 MPa, in agreement with the other studies. τ_0 and μ were calculated to be 12.5 MPa and 0.2, respectively. A large drop in the shear stresses as the thermal mismatch strain, $\Delta\alpha\Delta T$, between fibre and matrix exceeded ≈ 0.0025 was shown to be due to the formation of radial cracks around the fibres during processing [10, 11].

Despite the importance of temperature on the interfacial properties, as far as we are aware, no studies exist in which that relationship has been systematically explored *in situ*. The reason for this lack of data is not clear but could reflect one of the problems that we and others [9] have encountered in carrying out the single fibre pullout tests, namely the wide scatter in the results. Even though the test itself is relatively straightforward, scatter in the data can be so high as to mask other variables such as temperature. In some cases [8, 9] the scatter in τ was as high as 30–50%, even with specimens made in the same batch, let alone different batches. A second reason for the paucity of results is the fact that specimens in which epoxy is used to grip the fibres [10, 11] cannot be used at other than ambient temperatures. As described below, we have successfully measured the interfacial properties of the aforementioned systems, *in situ*, as a function of temperature. Both τ_d and τ_f were measured up to 510 °C.

2. Experimental procedure

The two glass compositions examined in this study were a soda-lime (Thomas Scientific) and a borosilicate (7740 Corning Glass). The fibre used was a carbon-coated (3 μm thick) SiC monofilament (Textron-SCS-6). The pertinent physical properties of the matrices and fibres used are listed in Table I. Since the main goal of this work was to investigate the effect of residual stresses on the interfacial properties, the matrices were chosen such that a wide range in thermal expansion coefficient mismatches existed between the two matrices and the fibres. However, the low radial expansion coefficient of the SiC fibre ensured that the radial residual stresses were compressive for both matrices.

The single fibre specimens were prepared based on a modification of the method developed by Coyle *et al.* [8]. The processing conditions are listed in Table II. A few fibres were sandwiched between two glass plates and placed in a ceramic mould. Molybdenum sheets (Morton Thiokol Inc., Danvers, MA) were placed on either side of the glass plates to avoid any reaction between the glass and the ceramic mould during fabrication. The whole assembly in turn was placed in a hot press (Series 3600, Vacuum Industries Inc., Somerville, MA). A dead weight ($\approx$ 23–37 KPa) was placed on the samples which were then heated at 6 °C min^{-1} to 725–800 °C, under vacuum, and held at temperature for 35–40 min. The dead weight was used to enhance the flow of the glass plates and ensure proper bonding between fibre and glass.

After the specimens had furnace cooled, the samples were cut into individual specimens each containing a single fibre and holes (8 mm diameter) were drilled in both plates with a diamond drill. Five to six specimens were fabricated per batch. The embedded lengths varied slightly from sample to sample but were kept in the range between 5–6 mm. The thicknesses of the glass sandwiches after fabrication are also shown in Table I.

Specimens were loaded in uniaxial tension on a screw driven Instron (Model 1172, Canton, MA). In order to facilitate specimen alignment during testing, swivel hooks with two ball joints were employed as

TABLE I Materials properties of SiC-glass composites

	SiC-monofilament (AVCO-SCS6)	Soda-lime glass (Thomas Scientific)	Borosilicate glass (Corning 7740)
Thermal. Exp. ($\times 10^{-6}C^{-10}$)	2.60 (longitudinal)[a] 2.53 (radial)[a]	8.90	3.20
E	410 GPa	69.0 GPa	62.8 GPa
G	170.8 GPa	28.5 GPa	26.1 GPa
Poisson's ratio	0.20	0.21	0.20
Strain point (°C)	–	465	520
Softening point (°C)	–	724	821
Dimension	143 μm diameter	1 × 1 × 0.19 cm	1 × 1 × 0.34 cm
Compositions	SiC with carbon coating	72% SiO_2 14% Na_2O 7.3% CaO 3.8% MgO 0.15% K_2O 0.05% FeO	80.5% SiO_2 13.0% B_2O_3 3.8% Na_2O 2.2% Al_2O_3 0.4% K_2O

[a] From [11].

TABLE II Fabrication conditions of SiC–glass composites

Parameter	SiC–soda-lime	SiC–borosilicate
Maximum temperature (°C)	725	800
Heating rate (°C min^{-1})	6.0	6.0
Holding time at max. temperature (min)	35	40
ΔT (°C)	440	495
Dead weight loading (KPa)	23–37	23–37
(p.s.i.)	16–27	16–27
Vacuum during heating (torr)	8×10^{-5} to 5×10^{-6}	

sample grips. Since the interfacial shear properties measured in single fibre pullout experiments similar to the ones reported here were found to be stressing rate dependent [10, 11], a constant crosshead speed of 8.5×10^{-6} m sec^{-1} was used.

In this study, τ_d and τ_f were calculated using Equations 1 and 2, i.e. as the pullout force divided by the fibre surface contact area. No attempt was made to study the effect of embedded length on τ, since Goettler and Faber [10, 11] have shown that for the SiC fibre used here, the relationship between debond load and embedded length was linear. However, in an attempt to gain some insight about the variations in frictional shear stress as pullout progresses, τ_f was calculated during the entire pullout length by dividing the load by the instantaneous embedded area. This area was, in turn, calculated from the instantaneous embedded length, which was directly read off the chart as shown in Fig. 1; it is simply the difference between total embedded length (OA) and the pullout length (O′A′) on the axis of displacement. In some of our preliminary runs the fibre pullout distance was measured using a travelling microscope and compared to that obtained from the chart. A satisfactory agreement between the two was found.

For the high temperature tests, the specimens were heated in a vertical furnace (Model E4, Research Inc., Minneapolis, MN) attached to the Instron. A thermocouple in contact with the specimen was used to measure the temperature. The specimens were heated to various temperatures at about 10–15 °C min^{-1} and held at temperature for 15–20 min prior to testing. A minimum of three specimens were tested at each temperature.

One of the limitations of the aforementioned technique is that it is quite time consuming. In order to speed up the process an alternative technique was developed by which the temperature dependence of the frictional stress, τ_f, was measured on a single specimen in a single run as follows: a 1/4 to 1/3 of the total embedded length was pulled out at room temperature at which point the load was released, after which the specimen was heated, held at temperature for 15 min, and then pulled. Once the sample started slipping, the load was again relaxed, and the process was repeated at a higher temperature. The load was relaxed during heating to prevent any possible fibre slip as the temperature was increased.

The fibre–matrix interfaces were examined under the SEM before and after pullout. Sections normal to the fibre axis were examined as well as some of the pulled out fibre surfaces and their corresponding empty glass matrix shells. The latter were examined by fracturing the glass plates along the thin cross sections.

3. Results

The most notable feature of the load displacement results, shown in Fig. 1, is the presence of a load maximum followed by a precipitous drop in load, which in turn is followed by a more gradual, serrated continually decreasing load. The presence of these serrations correlated well with a high value of the interfacial stresses and we believe them to be indicative of the formation of a good interfacial bond.

As mentioned earlier one of the difficulties associated with single fibre pullout tests in general has been the wide scatter in the results. One of the main accomplishments of this work has been to narrow this scatter considerably as shown in Fig. 2a and b for both the soda-lime and the borosilicate matrices, respectively. The curves for both systems are quite similar and three regions can be identified. (i) A debond shear stress which is higher for the soda-lime (17.4 ± 1.1 MPa) than for the borosilicate (9 ± 1 MPa). These values for τ_d represent the average of over five samples, not all shown in Fig. 2. (ii) An extended region over which the frictional shear stress remains fairly constant. The frictional shear stresses shown in all subsequent figures correspond to the values in this region. The average τ_f is again greater for the soda-lime (13 ± 1 MPa) than for the borosilicate (7 ± 1 MPa). (iii) A third region where the shear stress increases with decreasing embedded length.

The temperature dependence of both τ_d and τ_f are shown in Fig. 3a and b for the soda-lime and the borosilicate matrices, respectively. Initially, both τ_d and τ_f are found to decrease linearly with temperature. Replotting the data as function of thermal mismatch strain (Fig. 4a and b) yields the following straight lines:

$$\tau_d = 6.4 + 0.0227\Delta T (\mathrm{MPa}) \quad (0\text{–}450\,^\circ\mathrm{C}, \text{ soda-lime}) \qquad (6)$$

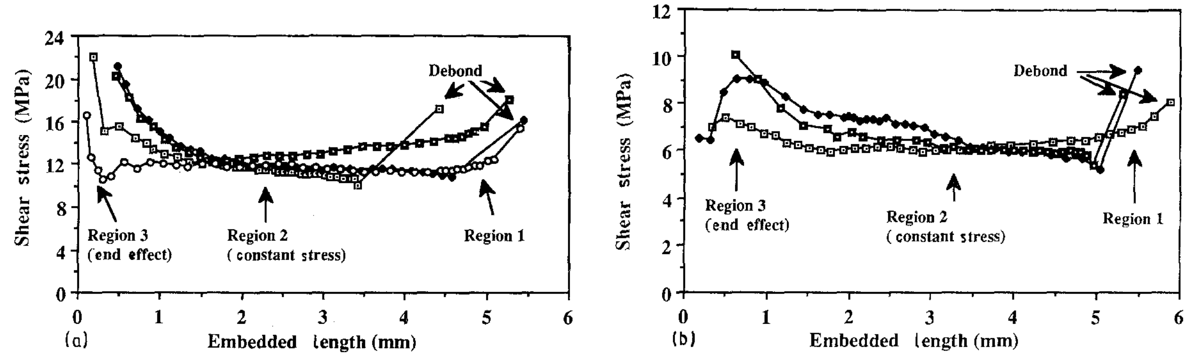

Figure 2 Debonding and frictional shear stresses against embedded length for (a) C-coated SiC–soda-lime matrices and (b) C-coated SiC–borosilicate matrices tested at 25 °C.

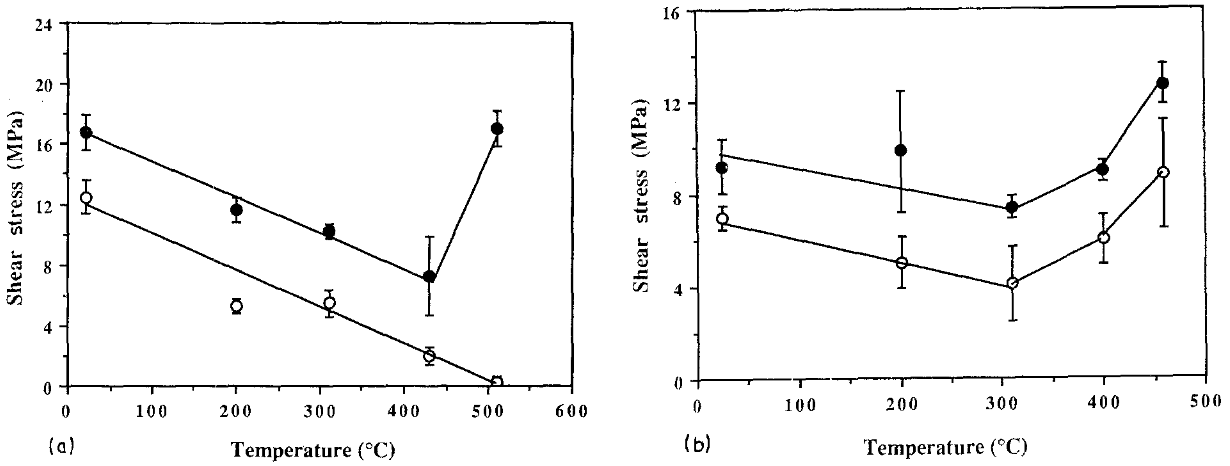

Figure 3 The temperature dependence of τ_d (●) and τ_f (○) for (a) SiC–soda-lime glass system and (b) SiC–borosilicate glass system. Every data point represents the average of three to five test specimens.

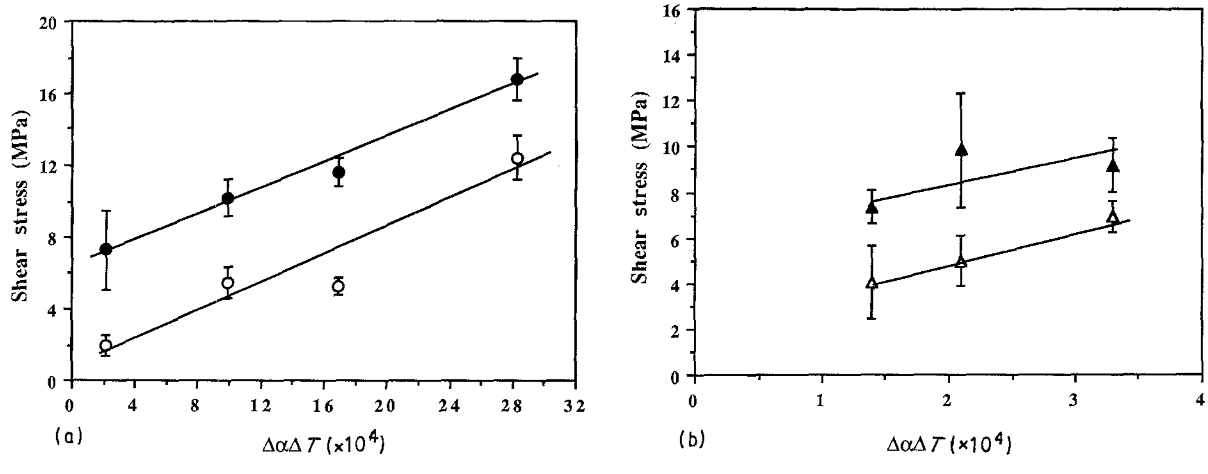

Figure 4 Relationship between τ_d (●) and τ_f (○) and the thermal expansion mismatch $\Delta\alpha\Delta T$ for (a) SiC–soda-lime specimens and (b) SiC–borosilicate specimens.

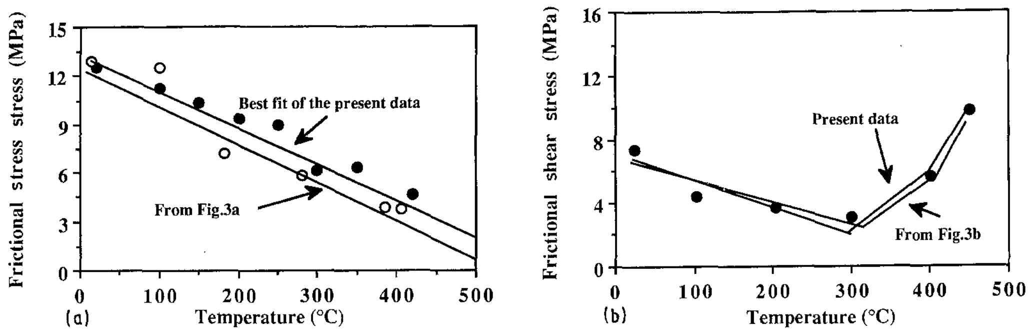

Figure 5 Comparison of data obtained from single specimen to that obtained from multiple specimens for (a) SiC–soda-lime and (b) SiC–borosilicate glass specimens.

and

$$\tau_d = 6.9 + 0.0056\Delta T(\text{MPa})$$

$$(0\text{–}300\,^\circ\text{C, borosilicate}) \qquad (7)$$

where $\Delta\alpha$ is included in the slope. ΔT is the $T_s - T_{test}$ where T_s is the matrix strain point and T_{test} the test temperature. (Equations 6 and 7 are only valid in the temperature range indicated.)

In both cases a minimum is observed. The location of the minimum and the nature of the load displacement curves beyond 300 °C varied, however. For the soda-lime system beyond $\approx 450\,^\circ\text{C}$, τ_f goes to zero, while τ_d almost doubles. For the borosilicate matrix, on the other hand, both τ_d and τ_f increase beyond $\approx 300\,^\circ\text{C}$ (Fig. 3b).

The temperature dependence of τ_f measured using single specimens are shown in Fig. 5a and b, for the soda-lime and the borosilicate matrices, respectively. Also reproduced in Fig. 5, for comparative purposes, are the results shown in Fig. 3a and b. The good agreement between the two sets of results is obvious.

4. Discussion

The results shown in Figs 2 to 5 clearly indicate the importance of temperature on the residual stresses and the effect of the latter on both the frictional and debonding shear stresses.

The residual thermal stresses can be estimated using the method of Oel and Frechette [15]. The radial compressive stresses at the fibre–matrix interface are calculated using the following relationship:

$$\sigma_r = \frac{E_f E_m}{E_m(1 - \nu_f) + E_f(1 + \nu_m)} \Delta\alpha\Delta T$$

which gives the residual stress at near the fibre–matrix interface for a thick sheath. The residual stresses are:

$$\sigma_r = 0.324\Delta T \qquad (\text{soda-lime}) \qquad (8)$$

and

$$\sigma_r = 0.032\Delta T \qquad (\text{borosilicate}) \qquad (9)$$

for the soda-lime and borosilicate matrices, respectively. At room temperatures these stresses are ≈ 142 and ≈ 16 MPa, respectively. The critical flaw associated with the former is of the order of 9 μm and it is thus not surprising that radial cracks were observed in the soda-lime matrices (Fig. 6). These radial microcracks extend 4 to 6 fibre radii and are usually, but not always normal to the original glass sandwiching interface. Their presence relieves the residual stresses and results in a reduction of the shear stresses needed for fibre pullout. This observation is in complete accord with that of Goettler and Faber [10, 11] who observed similar radial cracks when $\Delta\alpha\Delta T$ exceeded ≈ 0.0025. $\Delta\alpha\Delta T$ for the soda-lime is ≈ 0.0003.

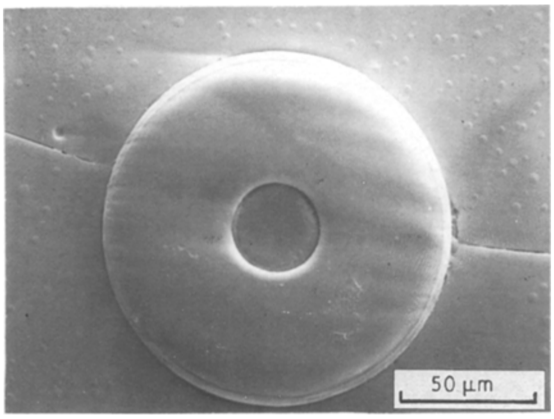

Figure 6 SEM micrograph of the radical cracks resulting from thermal expansion mismatch in SiC–soda-lime composite.

By combining Equations 5, 7 and 9, μ for the borosilicate matrix is calculated to be 0.18 which is in good agreement with the value of 0.2 obtained by Goettler and Faber [10, 11] for a similar system. Implicit in the calculation is that μ is not a function of temperature, which is a reasonable assumption as long as the test temperature does not exceed the glass transition temperature of the matrix.

The agreement between τ_0 measured in this work 3.5 ± 1 MPa (calculated by averaging the difference between τ_d and τ_f) and that measured by Goettler and Faber [10, 11] (12.5 MPa) is less satisfactory, however. The reason for the discrepancy is not clear, but could reflect variations in glass or fibre chemistries.

A similar calculation for the soda-lime system, assuming no cracks, yields a μ of 0.07 which is unreasonably low and indirectly confirms the presence of the cracks. If it is assumed that μ for soda-lime is of the same order as that for the borosilicate (i.e. ≈ 0.2), σ_r is calculated to be ≈ 32 MPa at room temperature.

The increase in the resistance to pullout beyond 300 °C for the borosilicate matrix is not entirely clear, but is most probably due to a reaction between the

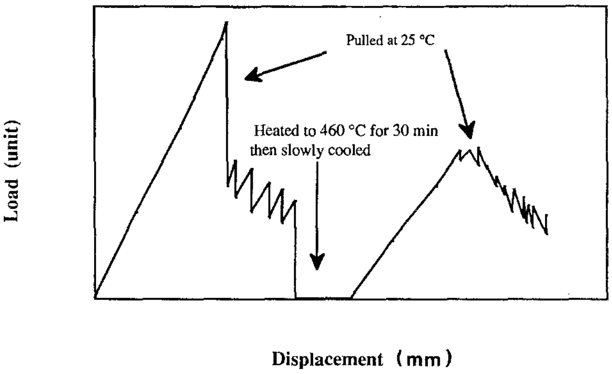

Figure 7 Effect of heating (30 min at 460 °C) on the load against displacement of a SiC–borosilicate glass after the fibre was debonded at room temperature.

fibre and matrix. To confirm that the increases in the shear stresses were due to a chemical reaction, and thus irreversible, as opposed to a thermal expansion anomaly, for instance, which would be recoverable after temperature cycling, the following experiment was carried out: a fibre was partially pulled out of the borosilicate matrix at room temperature, the load was released, the specimen heated to 460 °C for 30 min, and cooled. Upon reloading an increase in τ_f was observed as shown in Fig. 7.

It is well established in the literature [10, 11, 16] that replacement of the C-coating on SiC fibres by a silica layer results in enhanced bonding between fibre and matrix. The reaction sequence is believed to be the oxidation of the carbon layer originally present on the fibres to CO, followed by the oxidation of the underlying SiC to form an SiO_2 layer whose volume is greater than the original carbon layer and which bonds readily to the glass or glass–ceramic matrices.

We do not believe this to be the operative mechanism in our case for the following reasons: (i) The oxidation kinetics of SiC in the temperature range 300–500 °C are too sluggish to replace a 3 μm C-layer with silica. (ii) Examination of the fibres after pullout at elevated temperatures clearly shows the presence of the original C-layer (Fig. 8a and b).

An alternate reaction scheme, which is thermodynamically favourable [17] is:

$$Na_2O + C + O_2 \rightarrow Na_2CO_3$$
$$(\Delta G^\circ \text{ at } 700\,K = -933.9\,kJ\,mol^{-1})$$

where the Na_2O dissolved in the glass reacts with the carbon layer in the presence of ambient oxygen to form Na_2CO_3. Assuming the equilibrium oxygen partial pressure at 700 K at the interface can be taken to be that which is in equilibrium with carbon, which at 700 K is $\approx 3 \times 10^{-25}$ Pa, it follows that for activities of Na_2O greater than 7×10^{-36} Pa the reaction as written would proceed to the right. Higher oxygen partial pressures would increase the driving force even further. If indeed a carbonate layer does form, the presence of which would have to be substantiated using microchemical analyses, it would explain the increase in τ_d and τ_f observed at higher temperatures. It should be pointed out, however, that several unsuccessful attempts were carried out to try and form the carbonate by mixing the borosilicate glass powders with graphite and heating in air (up to 24 h at 400, 500 and 700 °C). The only crystalline compound detected in the X-ray diffraction patterns after the heat treatment was graphite. While it is conceivable that the extent of reaction could be so low as to be undetectable by X-ray diffraction it is unlikely.

It is generally reported that the SiC fibres used here are coated with 3 μm C-layer. However, Auger analysis (supplied by the manufacturer) of the surface of these fibres, indicates the presence of about 20 at % Si on the surface. This fact suggests an alternate mechanism for the increase in bonding at higher temperatures, namely the oxidation of this Si_xC surface layer during pullout to form a silica rich layer that would readily bond to the matrix. Indirect evidence for the importance of the role of oxygen and silicon comes from two sets of experiments we carried out. In the first set, the fibres were preoxidized at 700 °C for 30 min prior to fabrication of the single fibre specimens. This resulted in the formation of such a strong bond between the fibre and matrix that the fibres broke rather than pulled out. The load at which the fibres broke corresponded to a tensile stress of 1.8 GPa and a τ_d of at least 70 MPa. The non-oxidized fibre strength was measured to be 2 GPa. Had the surface been pure carbon, such an oxidative pretreatment would not have affected τ_d; only the pres-

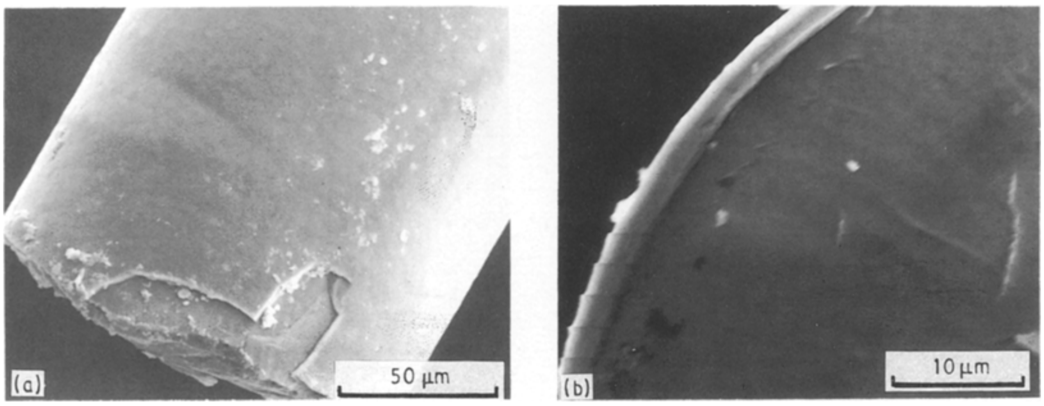

Figure 8 (a) Side view of fibre surface after pullout from a soda-lime specimen. (b) Same fibre viewed parallel to fibre direction. The carbon layer is still intact after pullout at elevated temperatures.

ence of an oxygen-rich silicon surface layer could explain the resultant enhanced bonding.

The second set of experiments involved heating the fabricated pullout samples in air (460 °C, 30 min) prior to testing. An increase in both τ_d and τ_f was observed. When the samples were heated in vacuum no increase was observed. This result is again consistent with the model proposed.

The aforementioned hypothesis could also explain the lack of reproducibility in the values of τ_d measured by various investigators. Slight variations in the surface Si/C as well as variations in the oxygen partial pressure during processing could result in very different surface chemistries and concomitant variation in τ_d.

Despite our best efforts to obtain a well bonded, defect free interface, the micrographs of the empty shells in which the fibres were embedded, shown in Fig. 9, clearly indicate that the interface is far from perfect. It appears that bubbles are trapped at the fibre–matrix interface. These bubbles could have formed as a result of various matrix–fibre reactions or as a result of partial oxidation of the carbon coating during processing. The presence of these defects is probably the main reason for the scatter in τ_d referred to earlier and could be the reason for the discrepancy between our results and those of others who have measured lower values for τ_d for the SiC–borosilicate system [8–11]. It is worth noting that these bubbles are very difficult to detect if the matrix–fibre interface is viewed normal to the fibre axis. The presence of these flaws also provides a ready path for the oxygen to diffuse down the fibre length.

The results obtained using the single specimen are comparable with those obtained using the multiple specimens. One disadvantage of measuring the interfacial properties in a single run is the fact the information concerning τ_d is lost. However since theoretically (i.e. Equation 5) and experimentally (Fig. 3) the difference between τ_f and τ_d, i.e. τ_0, appears to be a constant independent of temperature, it is possible to obtain the temperature variations of both τ_f and τ_d in a single run. It is to be noted that this technique can only be used if τ_f is relatively independent of embedded length over a wide enough range.

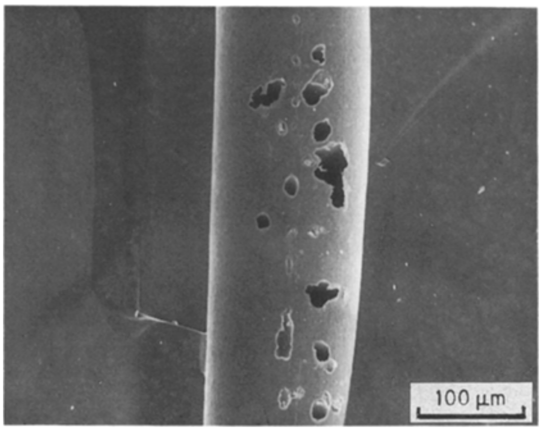

Figure 9 The longitudinal cross-sectional view of a matrix shell pulled at 430 °C. The same morphology was found to be independent of temperature.

5. Conclusions

The interfacial properties of two glass–SiC fibre systems were measured *in situ* in the temperature range 25–510 °C. Initially both the debond and frictional shear stresses were found to decrease linearly with temperature as a result of the relaxation of the compressive residual stresses developed during processing. The stress free debonding shear stress for the borosilicate matrix was found to be 3.5 ± 1 MPa and the friction coefficient between the carbon-coated fibre and the borosilicate matrix was calculated to be 0.18. At higher temperatures the debonding and frictional shear stresses were observed to increase as a result of the oxidation of the fibres. The large thermal expansion mismatch between the soda-lime matrix and the SiC fibres resulted in radial cracking of the former during processing.

Acknowledgements

The helpful comments from Dr D. C. Cranmer and Dr S. W. Freiman at the National Institute of Standard and Technology is gratefully acknowledged. This work was funded by the Office of Naval Research under contract number N0014-86-0096.

References

1. D. B. MARSHALL and A. G. EVANS, *J. Amer. Ceram. Soc.* **68**(5) (1985) 225.
2. C. W. GRIFFIN, S. Y. LIMAYE, D. W. RICHERSON and D. K. SHETTY, *Ceram. Eng. Sci. Proc.* **9**(7, 8) (1988) 671.
3. D. B. MARSHALL, *J. Amer. Ceram. Soc.* **66** (1984) C259.
4. J. F. MADELL, D. H. GRANDE, T. H. TSIANG and F. J. McGARRY, in "Composites Materials: Testing and Design", ASTM STP 893, edited by J. M. Whitney (ASTM, Philadelphia, 1986) pp. 87–108.
5. D. C. CRANMER, U. V. DESHMUKH and T. W. COYLE, "Symposium on Thermal-mechanical Behavior of Metal Matrix and Ceramic Matrix Composites", ASTM TP 1080 Atlanta, GA, 7 November, 1988 (ASTM, Philadelphia, PA, 1988) pp. 124–135.
6. R. J. KERANS, R. S. HAY, N. J. PAGANO and T. A. PARTHASARTHY, *Ceram. Bull.* **68**(2) (1989) 429.
7. F. J. McGARRY and D. W. MARSHALL, "Research on Wire-Wound Composite Materials", in "Symposium on Standards for Filament-Wound Reinforced Plastics", ASTM STP 327, ASTM, Philadelphia, PA, 1963, pp. 133–145.
8. T. W. COYLE, H. M. CHAN and U. V. DESHMUKH, "Interfaces in Polymer, Ceramics, and Metal Matrix Composites", edited by Hatsuo Ishida (Elsevier, 1988) pp. 489–501.
9. U. V. DESHMUKH and T. W. COYLE, *Ceram. Eng. Sci. Proc.* **9**(7–8) (1988) 627.
10. R. W. GOETTLER and K. T. FABER, *ibid.* **9** (7–8) (1988) 861.
11. *Idem, Composites Sci. Technol.* **37** (1989) 129–147.
12. P. LAWRENCE, *J. Mater. Sci.* **7** (1972) 1.
13. R. J. GRAY, *ibid.* **19** (1984) 861.
14. J. AMIRBAYAT and J. W. S. HEARLE, *J. Fiber Sci. Tech.* **2** (1970) 223.
15. H. J. OEL and V. D. FRECHETTE, *J. Amer. Ceram. Soc.* **69** (4) (1986) 342.
16. M. D. THOULESS, O. SBAIZERO, L. S. SIGL and A. G. EVANS, *ibid.* **72**(4) (1989) 525.
17. JANAF Thermochemical Table, 3rd edn., U.S. National Bureau of Standards, 1986.

Received 14 November
and accepted 1 December 1989